Polymer 51 (2010) 5539–5549

Contents lists available at ScienceDirect

Polymer

journal homepage: www.elsevier.com/locate/polymer

Role of boric acid for a poly (vinyl alcohol) film as a cross-linking agent: Melting behaviors of the films with boric acid

Tsukasa Miyazaki*, Yuuki Takeda, Sachiko Akane, Takahiko Itou, Akie Hoshiko, Keiko En

Functional Design Technology Center, Nitto Denko Corporation, 1-1-2, Shimohozumi, Ibaraki, Osaka 567-8680, Japan

ARTICLE INFO

Article history:
Received 17 May 2010
Received in revised form
17 August 2010
Accepted 15 September 2010

Keywords:
Melting of semi-crystalline polymers
Cross-linking agent
Simultaneous SAXS/WAXD measurements

ABSTRACT

We have investigated the role of boric acid as a cross-linking agent for a poly (vinyl alcohol) (PVA) film when the film is immersed in boric acid aqueous solution. DSC results show that the films with boric acid exhibit the higher glass transition temperatures than that of the PVA film without boric acid, when the films are dried after immersing in boric acid aqueous solutions with various boric acid concentrations, implying that boric acid penetrating into the films slows down the PVA molecular motion. Furthermore, simultaneous small-angle X-ray scattering and wide-angle X-ray diffraction measurements were performed on the melting processes of the PVA films with boric acid. We found that the crystallite size increase originated from melting and recrystallization do not occur for the PVA films with boric acid, whereas in the case of the PVA without boric acid the crystallite size is enlarged in both directions parallel and perpendicular to the chain axis via melting and recrystallization on melting. These indicate that chemical reactions of boric acid to the PVA molecular chains in amorphous regions resulted in cross-linking points take place in boric acid aqueous solutions, inhibiting recrystallization on melting, because the cross-links slow down the PVA molecular motion and must not be included in the crystalline domains.

1. Introduction

Poly(vinyl alcohol) (PVA) has been widely used in various industrial applications such as high strength fibers, biodegradable materials and so on [1,2]. In particular, this material has been substantially available to a polarizer with the extremely high dichromatic performance in accordance with the recent development of liquid crystalline displays.

We have systematically investigated the microscopic structural changes of a PVA film during processing the polarizer for understanding the relationships between microstructural changes of the film and the high dichromatic performance [3,4]. In our previous papers, we elucidated the microstructural changes of this film during uniaxial stretching in water by conducting the simultaneous stress–strain and small-angle X-ray scattering measurements [3], and the stress–strain and wide-angle X-ray diffraction ones [4]. In result, we found that the oriented amorphous regions are developed among the adjacent microfibrils on the film stretching [3]. It was suggested that PVA–iodine complexes with an ability of the high dichromatic performance are formed in the oriented amorphous regions among the microfibrils associated with the film stretching.

In the practical processes, boric acid has been added to the solution used in the film stretching, promoting the formation of PVA–iodine complexes in the film [5,6]. Boric acid plays the crucial role on the production of high performance polarizers. However, it is not clear why boric acid additive improves the dichromatic performance of a polarizer based on this film, although this is considered to be due to the increase in the amount of the complexes, and the degree of orientation of ones. It is expected that boric acid plays a role as a cross-linking agent for PVA by immersing the film in boric acid aqueous solution. The chemical structures associated with the reaction of boric acid to the PVA molecular chains have not been also declared, although the various reaction schemes and the chemical structural models have been proposed for understanding the role of boric acid as a cross-linking agent [7,8].

In this paper, we investigate the role of boric acid penetrated into the PVA film when the film is immersed in boric acid aqueous solutions. First, we performed DSC measurements for the films dried after immersing in boric acid aqueous solutions with various boric acid concentrations, found that boric acid slows down the PVA molecular motion. Second, we observed melting processes of the PVA films with various boric acid concentrations by

* Corresponding author. Tel.: +81 72 621 0265; fax: +81 72 621 0316.
E-mail address: tsukasa_miyazaki@gg.nitto.co.jp (T. Miyazaki).

0032-3861/$ – see front matter © 2010 Elsevier Ltd. All rights reserved.
doi:10.1016/j.polymer.2010.09.048

simultaneous small-angle X-ray scattering (SAXS) and wide-angle X-ray diffraction (WAXD) measurements. It was found that boric acid hinders recrystallization of the PVA molecules in amorphous regions on melting. These behaviors indicate that boric acid reacts to the PVA molecules in the amorphous regions intermediated among the lamellar crystallites and the lamellar stacks, cross-linking the PVA chains in these regions. As a result, it was suggested that boric acid plays an important role on the effective orientation of a large amount of PVA molecular chains without strain-induced crystallization as the cross-linking agent during film stretching, as the cross-linkers inhibit recrystallization of the PVA chains. In this paper, we do not refer to the chemical structure of the cross-linking points between boric acid and the PVA molecules. This will be subjected in the following papers.

2. Experimental

2.1. PVA films

The PVA films made from the PVA powder with the degree of polymerization of 2400 by Kuraray Co. were used in this study. The triad tacticity ($mm = 0.21$, $mr = 0.50$, $rr = 0.29$) was determined in solution state by ^{1}H NMR spectroscopy. The PVA also had a high degree of saponification, which is larger than 99 mol%. The thickness of the PVA films used was typically about 0.1 mm. Prior to use, the PVA films were further immersed in distilled water for eliminating residual additives, subsequently dried in an air-oven at 60 °C for 10 min. It was confirmed that no residual additive was included in the films used in this study by this process. PVA films with boric acid were constructed by immersing in boric acid aqueous solutions with various boric acid concentrations within 0–3 wt% for 3 min, followed by drying in an air-oven at 60 °C for 60 min again. The weight fractions of boric acid in the films with these treatments were investigated with an inductively coupled plasma mass spectrometer, plotted against those in the solutions for immersing in Fig. 1. The figure shows that the weight fraction of boric acid in the films increases with increasing the boric acid concentration in aqueous solutions.

In our previous paper, we elucidated that a part of PVA crystallites dissolves in water, when the film is immersed in aqueous solutions [4]. However, many crystallites remain in the film without dissolution or swelling with water. Therefore, boric acid is considered to exist in amorphous regions, because boric acid molecules must not penetrate into the crystalline sequences of the PVA chains.

2.2. Differential scanning calorimetry

Differential scanning calorimetry (DSC) measurements were performed using a Diamond DSC (Perkin–Elmer Co.) equipped with an intracooler 2P cooling accessory. The temperature and heat flow at the heating rate of 10 °C/min were calibrated using an indium and tin standard with nitrogen purging. Prior to the measurements, the PVA samples were further dried in a vacuum oven for 12 h at 60 °C for evaporating residual water in the films. After drying the films were immediately weighted and sealed in aluminum pans. Then the samples were heated from 20 °C to 250 °C at the heating rate of 10 °C/min. The reference material was an empty pan.

2.3. Simultaneous SAXS/WAXD measurements

Simultaneous SAXS/WAXD experiments on melting processes of the PVA films with and without boric acid were performed with the SAXS/WAXD apparatus at BL40B2 beamline of SPring-8 (Hyogo, Japan). The wavelength was turned at 0.1 nm. The camera lengths were 1803 mm and 64 mm for SAXS and WAXD experiments, respectively. The CCD detector system bearing an image intensifier and the CMOS detector (FlatPanel) were used to allow rapid acquisitions of two-dimensional (2-D) scattering patterns from the samples on heating and cooling for SAXS and WAXD experiments, respectively. The calibrations of the scattering angle were carried out by using diffractions from the regular structures in collagen obtained from chicken tendon and Si powder purchased from the National Institute of Standard Technology in USA for SAXS and WAXD experiments, respectively. Film samples with the thickness of about 0.1 mm were wrapped with an aluminum foil to ensure thermally homogeneous heating and cooling with the temperature controlled cell (Linkam THMS 699, Japan Hitech Co.). The films were heated from 50 °C to 250 °C (first heating run), immediately followed by the cooling ramp from 250 °C to 50 °C. For the PVA film without boric acid, the sample was heated again from 50 °C to 250 °C (second heating run). The heating and the cooling rates were 10 °C/min. 2-D scattering data were collected on all heating and cooling ramps with an acquisition time of 5 s at the interval of 15 s.

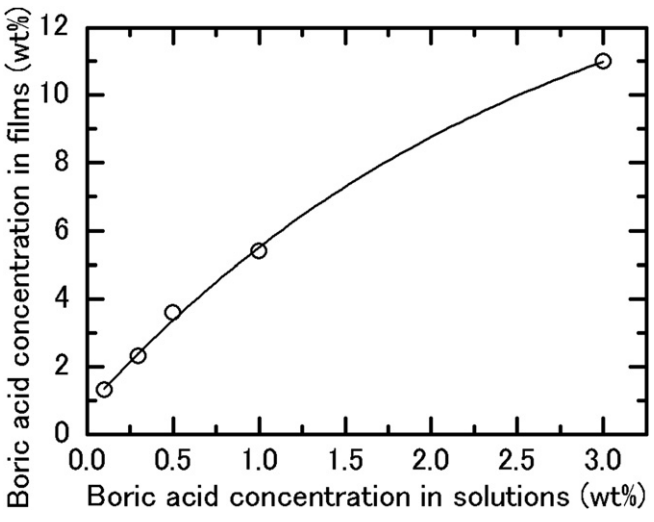

Fig. 1. Weight fractions of boric acid in the films dried after immersing in boric acid aqueous solutions with various boric acid concentrations.

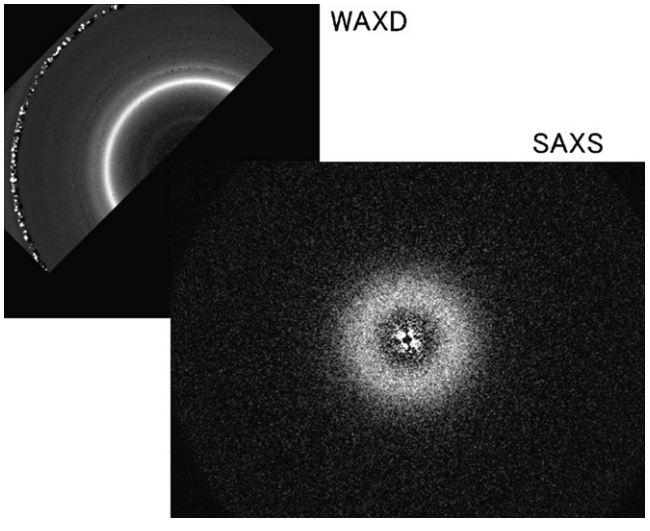

Fig. 2. 2-D SAXS and WAXD patterns for the PVA without boric acid at 50 °C prior to the heating ramp.

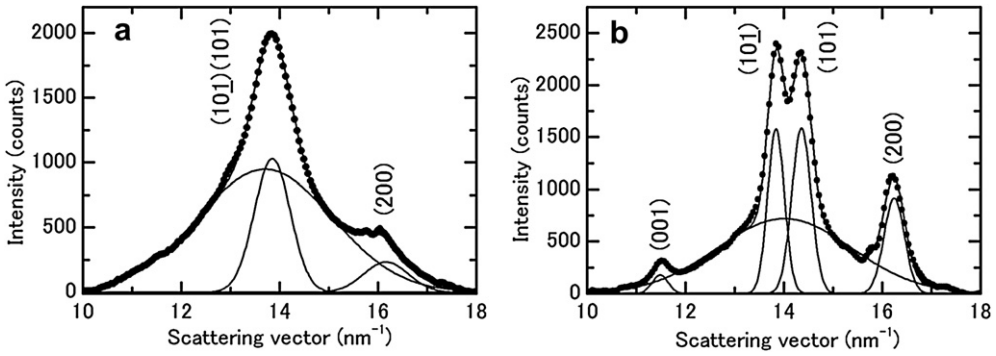

Fig. 3. Typical examples of the peak decompositions of the integrated 1-D intensity profiles for the 2-D WAXD pattern of the PVA without boric acid at 50 °C prior to first (a) and second heating runs (b). Lines are the best fitting curves. Points are experimental data.

3. Data analysis

3.1. WAXD

Typical 2-D SAXS and WAXD patterns obtained with SAXS and WAXD detectors as described above are shown in Fig. 2. In the WAXD image in Fig. 2, an outsider incontinuous Debye ring is ascribed to the aluminum foil with which the sample is wrapped for keeping the thermally homogeneous heating and cooling conditions.

For the SAXS path, WAXD diffraction patterns obtained with the FlatPanel detector were limited to selected area only, including the vertical and horizontal areas. Therefore, the one-dimensional (1-D) scattering profile was integrated within 45° from the vertical direction. Prior to the integration, air scattering pattern was subtracted from the patterns of samples taking into account of the transmittances of the samples. The integrated 1-D scattering profiles were corrected for the changes of Lorentz factor and the detector area according with the scattering angle.

The typical 1-D scattering profiles of the film at 50 °C prior to first and second heating runs are shown in Fig. 3a and b, respectively.

For determining the apparent crystallinity index, the peak decomposition procedures were performed on these 1-D profiles obtained on heating. For the samples on first heating run, 1-D scattering profiles are decomposed into two crystalline peaks ((101) (10$\bar{1}$) doublet and (200) planes) and one amorphous halo in the examined region (q = 10–18 nm^{-1}; the scattering vector q defined by $q = (4\pi/\lambda)\sin\theta/2$ with λ and θ being the wavelength of X-rays and the scattering angle, respectively). For the sample on second heating run, the decomposed peak fitting procedure was applied to the four crystalline peaks ((001), (10$\bar{1}$), (101) and (200)) and one amorphous halo in the same examined region for high crystallinity of the film crystallized non-isothermally from the melt (250 °C). The peak type was chosen to be Gaussian. In the peak fitting procedure, only one fixed parameter is the full width at half maximum (FWHM) of the amorphous peak, which can be evaluated from the scattering profile of the sample in a melt state. Other parameters (positions, heights and FWHMs of the two or four crystalline peaks, and position and height of the amorphous peak) are floated in the fitting routine. The apparent crystallinity index, f_c is thus determined as follows:

$$f_c = \frac{\sum A_c}{\sum A_c + A_a} \tag{1}$$

where A_c is the integrated area underneath the crystalline peaks and A_a is the integrated area of the amorphous peak [9–11]. Typical peak fitting results are also included in Fig. 3a, b, indicating that these fitting procedures can represent the experimental scattering profiles very well.

The lateral crystallite size of lamellae can be evaluated with the crystalline peak width by using the following Scherrer equation:

$$l_c = \frac{0.9\lambda}{(\Delta 2\theta)\cos\theta_m} \tag{2}$$

where $\Delta 2\theta$, θ_m, λ are the FWHM of the crystalline peak in radian, half of the peak angle and the X-ray wavelength, respectively. The (101) (10$\bar{1}$) doublet and (10$\bar{1}$) crystalline peaks were used for the samples on first and second heating runs, respectively (b-axis is defined to be parallel to the chain direction).

3.2. SAXS

1-D SAXS profiles can be circularly integrated from 2-D scattering patterns as shown in Fig. 2. Prior to the integration, air scattering pattern was also subtracted from the patterns of samples taking into account of the transmittances of the samples, such as that in the WAXD data analysis procedure as described above. The obtained 1-D profiles (scattering intensity $I(q)$ as a function of q) were further subjected to the so-called Lorentz correction, i.e., $q^2I(q)$ was plotted as a function of q.

The correlation function $\gamma(r)$ is calculated from the scattering intensity as

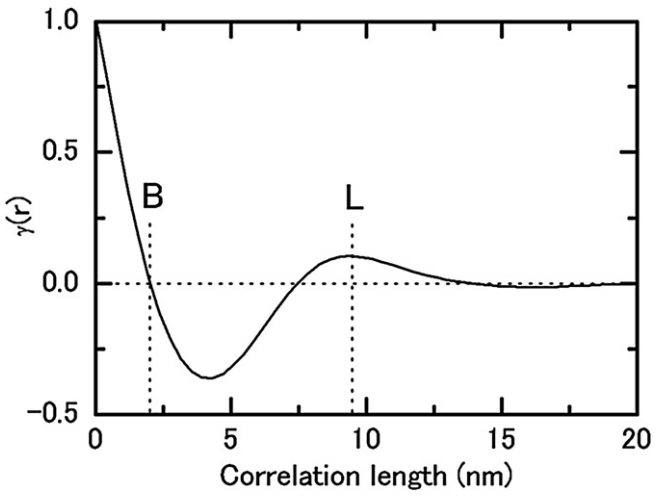

Fig. 4. Typical example of the 1-D correlation function for the PVA film without boric acid at 50 °C prior to first heating run. B is the first intercept with the line, $\gamma(r) = 0$. L is the first maximum in γ(r).

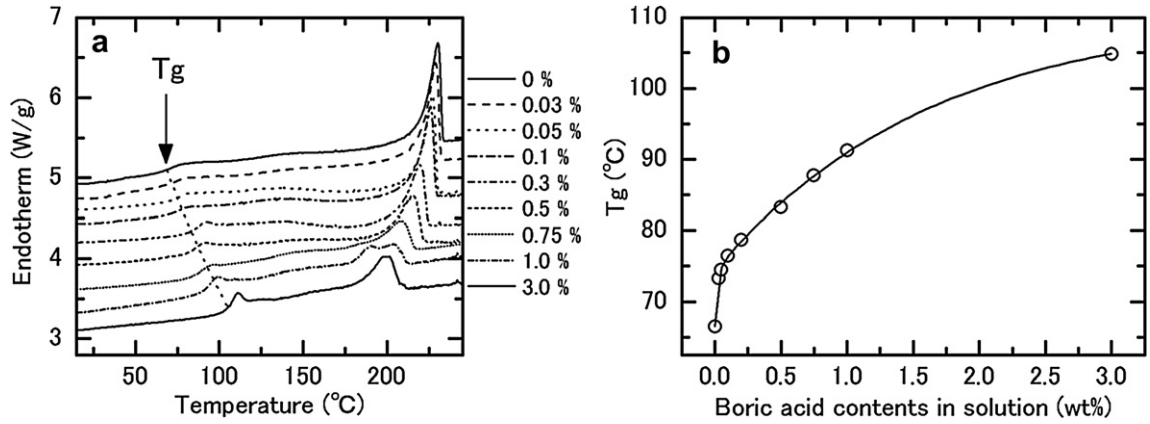

Fig. 5. (a) DSC endothermic curves for the PVA films containing boric acid by immersing in boric acid aqueous solutions with various boric acid concentrations shown in the figure. (b) *Tg*s for the PVA films with various boric acid concentrations shown in (a). The solid line in (b) is drawn to guide the eye.

$$\gamma(r) = \frac{\int_0^\infty (I(q) - I_b)q^2 \cos(q \cdot r)\mathrm{d}q}{Q} \tag{3}$$

where I_b is the background intensity profile. Q is the invariant defined as [9–18]

$$Q = \int_0^\infty (I(q) - I_b)q^2\mathrm{d}q \tag{4}$$

The background intensity profile (the liquid scattering profile) is derived from the Porod law at a higher q region as followed

$$I(q) = I_b + Pq^{-4} \tag{5}$$

where P is the Porod constant. Because of the finite q range of experimental SAXS data, extrapolation of the 1-D scattering profiles to both the low and the high q regions is necessary for the integration of the intensity profile, $I(q) - I_b$. Extrapolation of the 1-D scattering profiles to $q = 0$ was achieved by linear extrapolation, and extrapolation to large q can be accomplished by using the Porod law, $I(q) - I_b = P/q^4$, as described by Eq. (5). The typical example of the correlation function is shown in Fig. 4 for the PVA film without boric acid at 50 °C prior to first heating run. The long period values can be determined by the position of the first maximum, L in $\gamma(r)$. In addition to the long period, the linear degree of crystallinity, x within the lamellar stacks can be derived from the following equation:

$$x(1 - x)L = B \tag{6}$$

where B is the first intercept with the line, $\gamma(r) = 0$ in the figure. The x can have two values. Only Eq. (6) does not reveal which values represent the linear degree of crystallinity. The linear degree of crystallinity has to be determined in conjunction with other information, such as the bulk-volume degree of crystallinity. The minimum x of possible two values was selected to be the linear degree of crystallinity in this study, as mentioned below. The lamellar thickness Lc is then calculated as the product of L and x.

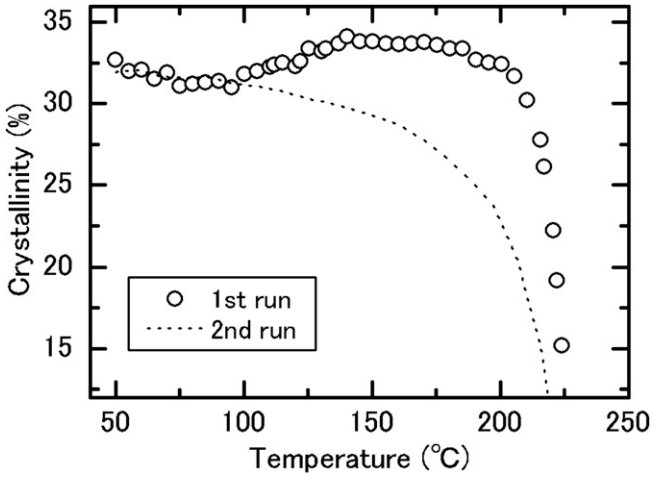

Fig. 6. Crystallinity indexes of the PVA film without boric acid on first (open circles) and second heating runs (dotted line). For comparison of both data obtained on first and second heating runs, the crystallinity indexes on second heating run are off-set by conducting the factor of 0.73.

4. Results

4.1. DSC results for the PVA films with boric acid

Fig. 5(a) shows the endothermic curves of the PVA films dried after immersing in boric acid aqueous solutions with various boric acid concentrations as indicated in the figure. The glass transition temperature, *Tg* of the film increases with the boric acid concentration in solution, as shown in Fig. 5(b), implying that the PVA chain motion becomes slow with increasing the boric acid concentration in the film as shown in Fig. 1. It is considered that boric acid cross-links the inter and intra molecular chains in amorphous regions associated with chemical reactions between the PVA chains and boric acid in solution as mentioned in Experimental section, consequently slowing down the molecular motion. Fig. 5(b) may show that the cross-linking density in the film increases moderately with boric acid concentration in solution up to 3 wt%. Moreover, the melting temperature decreases with increasing the boric acid concentration, as schematically shown in Fig. 5(a), probably indicating that larger crystallites, which are usually produced as a result of melting and recrystallization, do not grow in the films on the heating run. This may be also due to slow down of the molecular motion with cross-links. Furthermore, boric acid must hinder the crystallite growth in the direction parallel to the chain direction with cross-linking points nearby crystallites, because cross-linking points cannot be included in crystalline domains.

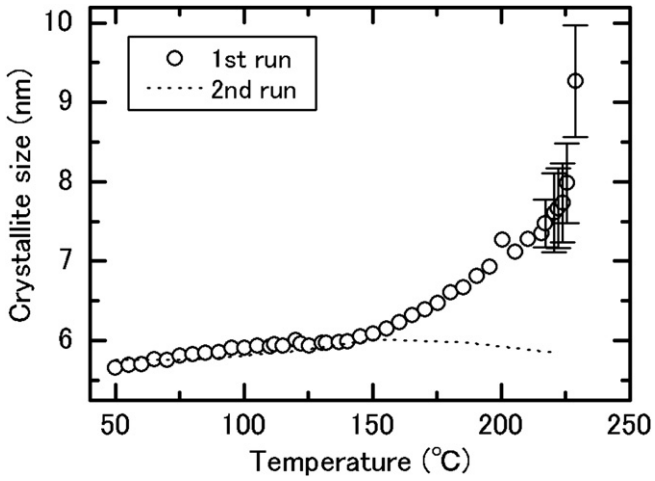

Fig. 7. Crystallite sizes of the PVA film without boric acid on first (open circles) and second heating runs (dotted line). For comparison of both data obtained on first and second heating runs, the crystallinity indexes on second heating run are off-set by conducting the factor of 0.50.

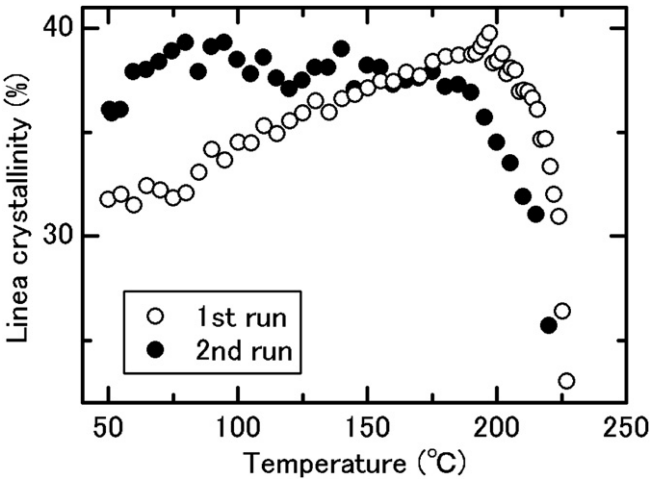

Fig. 9. Linear crystallinity within the lamellar stacks of the PVA film without boric acid on first and second heating runs.

4.2. Melting behaviors of the PVA without boric acid

The PVA film without boric acid has a high crystallinity index after first heating run compared to that prior to first heating run, as typically indicated in Fig. 3a and b. For the as-prepared sample the crystallinity index is found to be 33% with the WAXD technique. On the other hand, the apparent crystallinity index is 45% after first heating run, much larger than that prior to first heating run. This value is equivalent to that after second heating run, indicating that the sample after first heating run should not be degraded thermally. PVA is a thermally degradable polymer at a high temperature, in particular above the melting point. Therefore, for obtaining a PVA sample with high crystallinity, the material is hard to be isothermally crystallized below the melting point after keeping appropriately above the melting point [19,20], different from other industrially available polymers with relatively high crystallinity, which can be easily obtained with isothermal crystallization after fully melting for a long time. We attempted to obtain the sample with a higher degree of crystallinity by annealing the as-prepared samples at relatively high temperatures. However, we could not obtain the film with a higher crystallinity index compared to that after first heating run. Therefore, it may be suggested that the PVA used in this study has a fully high degree of crystallinity without thermal degradation on heating up to 250 °C by cooling immediately from this temperature at the heating and cooling rates of 10 °C/min.

Figs. 6 and 7 show the crystallinity indexes and the lateral crystallite sizes on first and second heating runs, respectively. On second heating run the change of the crystallinity index with temperature is starting from 45% at 50 °C compared to that starting from 33% on first heating run, as described above, and the lateral crystallite size is starting from 11.3 nm at 50 °C on second heating run compared to that starting from 5.7 nm on first heating run. For comparison of both data obtained on first and second heating runs, the crystallinity indexes and the crystallite sizes on second heating run shown in Figs. 6 and 7 are off-set by conducting the factors of 0.73 and 0.50, respectively. Figs. 8a, b and 9 indicate the long period, the lamellar thickness and the consequent linear crystallinity in the lamellar stacks on first and second heating runs, respectively. Fig. 10 shows the scattering invariant derived from Eq. (4) on first and second heating runs.

For the film on second heating run, that is to say, the PVA film with a fully high degree of crystallinity, the crystallinity index derived from the WAXD technique decreases moderately with temperature up to about 180 °C, as shown in Fig. 6. It seems that existing crystallites continue to melt in accordance with the size and/or perfection. However, the lateral crystallite size does not almost change with temperature up to the melting point. Moreover, the long period and the lamellar crystallite thickness increase gradually with temperature up to 180 °C, probably indicating that the lamellar stacks are only expanded thermally. Therefore, it is suggested that substantial structural changes, such as melting of existing crystallites, recrystallization, and melting and

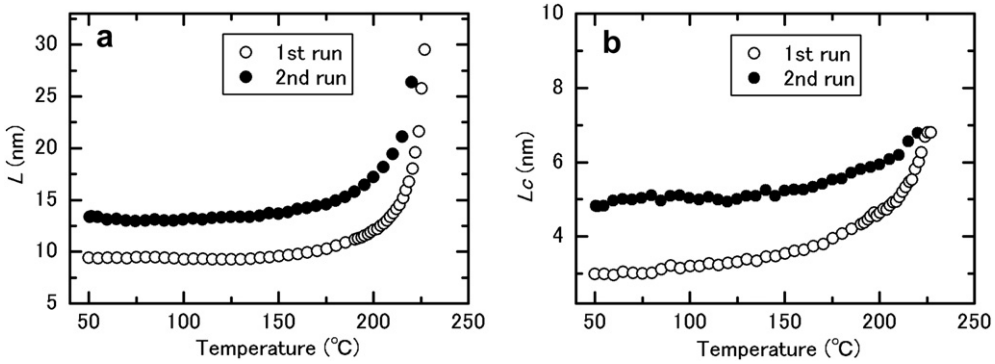

Fig. 8. Long period (a) and the lamellar thickness changes (b) of the PVA film without boric acid on first and second heating runs.

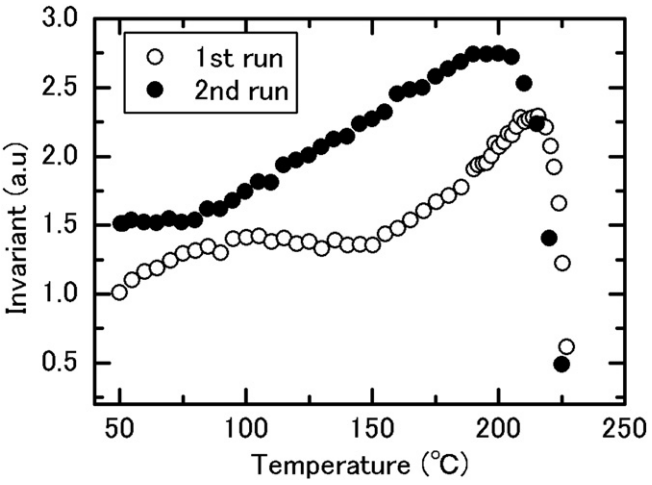

Fig. 10. SAXS invariants of the PVA film without boric acid on first and second heating runs.

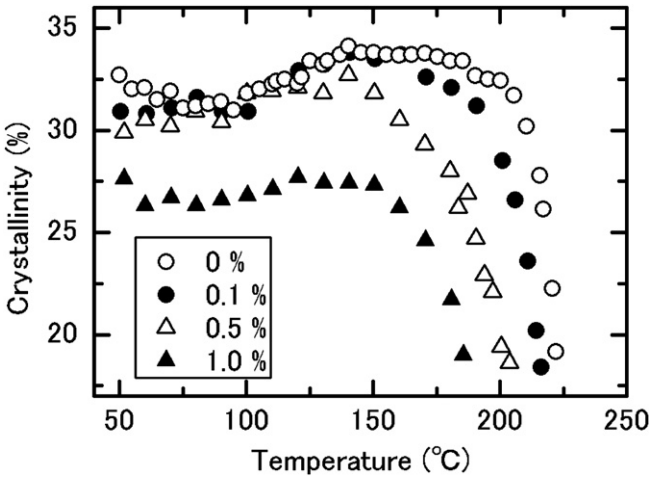

Fig. 11. Crystallinity indexes of the PVA films with various boric acid contents dried after immersing in aqueous solutions with various boric acid concentrations shown in the figure.

recrystallization do not occur up to 180 °C. The scattering invariant changes linearly at both sides of about 75 °C on second heating run (Fig. 10). The break at 75 °C should be ascribed to *Tg* of the film [17,21]. The scattering invariant, *Q* is given by:

$$Q = K\phi_s\phi_c(1-\phi_c)(\rho_c-\rho_a)^2 \quad (7)$$

where *K*, ϕ_s, ϕ_c, ρ_c, and ρ_a are constant, the volume fraction of lamellar stacks, the linear crystallinity in the lamellar stacks, the density of crystallites and that of amorphous regions, respectively. As mentioned above, if substantial structural changes do not occur below 180 °C, *Q* is dominated only with the difference of the thermal expansion coefficients between amorphous regions intermediated among crystallites and crystalline lamellae, as described with Eq. (7). Below *Tg*, the difference of the thermal expansion coefficients between amorphous regions and crystalline lamellae is much smaller than that above *Tg*, leading to linear increases in *Q* at both sides of *Tg* with a smaller linearity constant below *Tg* and a larger one above *Tg*. In fact, as shown in Fig. 10, the linear increases in *Q* with a break at 75 °C are observed below 180 °C, also indicating that substantial structural changes do not occur below 180 °C except the thermal expansions of amorphous regions and crystallites. The thermal expansion of the lamellar stacks without structural changes can also explain the linear decrease in the linear crystallinity within the lamellar stacks with a small linearity constant below 180 °C (Fig. 9), as a result of a larger thermal expansion coefficient of amorphous regions than that of crystalline lamellae.

These behaviors imply that the PVA film on second heating run does not go through large structural changes, such as recrystallization, rearrangement of existing crystallites, melting of smaller and/or imperfect crystallites, and melting and recrystallization except the thermal expansion of crystallites and amorphous regions below 180 °C. Therefore, below 180 °C, the moderate decrease in the crystallinity index derived from WAXD should be attributed to the thermal atomic vibrations of increasing amplitude in the molecular chains in crystallites, so-called Debye–Waller factor [21], not ascribed to the melting of existing crystallites in accordance with the size and/or perfection.

As shown in Fig. 6, above 180 °C the steep decrease in the WAXD crystallinity index is observed without the lateral crystallite size changes (Fig. 7), as a final melting process. The steep increases in the long period and the tiny increase in the lamellar thickness are also observed above 180 °C as shown in Fig. 8a and b, accompanying with the resultant steep decrease in the linear crystallinity within the lamellar stacks (Fig. 9). A tiny lamellar thickness increase must be attributed to the melting of relatively smaller crystallites in the lamellar stacks rather than the lamellar thickening with temperature, because the apparent crystallinity and the linear crystallinity observed with WAXD and SAXS, respectively, decrease steeply above 180 °C. Therefore, above 180 °C it is considered that the existing crystallites in the lamellar stacks merely melt with increasing temperature without the lateral growth of crystallites (Fig. 7) and the lamellar thickening (Fig. 8b). The consequent steep decrease in the linear crystallinity within the lamellar stacks on melting also implies that the choice of *x* in Eq. (6) as the linear crystallinity must be reasonable, as mentioned in Data analysis section.

Both WAXD and SAXS data suggest that for the PVA without boric acid on second heating run large structural changes, such as melting and recrystallization do not occur below 180 °C except the thermal expansions of amorphous and crystalline regions, and existing crystallites are merely melting in accordance with the size and/or perfection with temperature above 180 °C. In particular, even in the vicinity of the final melting point (above 200 °C) accompanied with the substantial decreases in the apparent crystallinity and the linear crystallinity within the lamellar stacks, the crystallite sizes do not substantially change in both directions parallel (the lamellar thickness shown in Fig. 8b) and perpendicular to the chain direction (the lateral size of crystallites shown in Fig. 7) with temperature on second heating run, clearly indicating that merely melting of existing crystallites occur without melting and recrystallization even near the melting point, as expected for a film with fully high crystallinity. Of course, gradual melting of the existing crystallites with relatively smaller sizes and imperfectness must be considered with temperature even below 180 °C. However, we should conclude that if there are any lamellae melting in the lamellar stacks on second heating run, their number must be extremely small and may be neglected below 180 °C.

On the other hand, large structural changes are observed on first heating run, as shown typically in Fig. 6. Below 100 °C, the apparent crystallinity index decreases nominally owing to the thermal atomic vibrations, as mentioned above. However, the apparent crystallinity index in the film increases above 100 °C on first heating run, as compared to that on second heating run, implying that the processes of recrystallization and/or rearrangement of existing crystallites take place dominantly above 100 °C on first

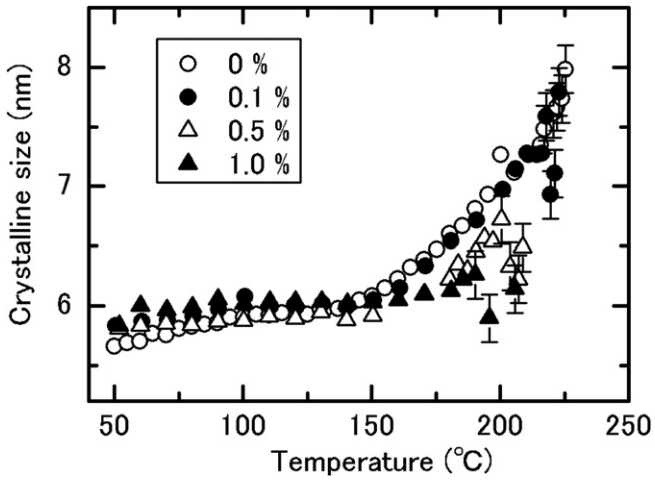

Fig. 12. Crystallite sizes of the PVA films with various boric acid contents dried after immersing in aqueous solutions with various boric acid concentrations shown in the figure.

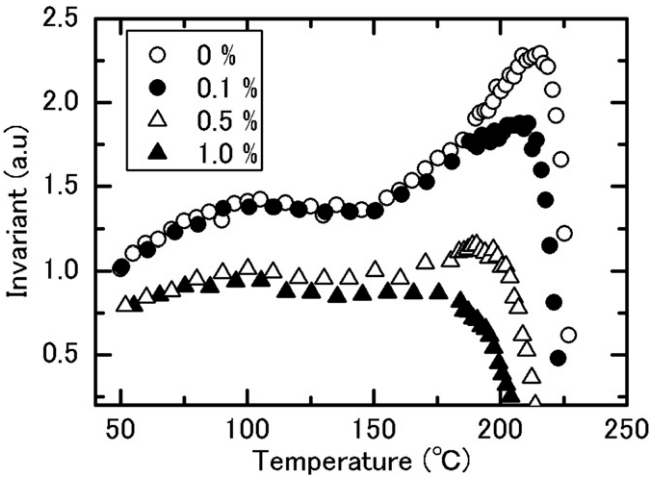

Fig. 13. SAXS invariants of the PVA films with various boric acid contents dried after immersing in aqueous solutions with various boric acid concentrations shown in the figure.

heating run, although neglectable smaller or disorder crystallites should be also considered to continue to melt above 100 °C. In the temperature domain below 150 °C, however, recrystallization and/or rearrangement of existing crystallites should not accompany with the increase in the crystallite size, because the lateral crystallite size remains constant and the substantial increase in the lamellar thickness does not occur, as shown in Figs. 7 and 8b. It is difficult to explain the changes in the scattering invariant below 150 °C, and the increase in the linear crystallinity within the lamellar stacks above 80 °C, at which recrystallization and/or rearrangement of existing crystallites must not occur yet, as shown in Figs. 9 and 10 without taking into account of water evaporation out of the film. We will attempt to explain these behaviors in the light of water evaporation in Discussion section.

Above 150 °C, melting and recrystallization must take place with the increase in the crystallite size on heating, because the crystallite size begins to increase steeply in the lateral direction of crystalline lamellae (Fig. 7) and in the direction parallel to the chain direction (the lamellar thickness; Fig. 8b) with temperature. This increase in the lamellar thickness may be explained with the thickening of existing lamellae only. However, above 150 °C the lamellar thickness increase is accompanied with the long period increase, as shown in the expanded views of Fig. 8a and b (Figs. 14b and 18). Therefore, above 150 °C merely thickening of existing lamellae should be ruled out as the explanation of the steep increase in the lamellar thickness. The steep increases in the lamellar thickness and the long period may be also explained with merely melting of relatively smaller and/or imperfect crystallites in the lamellar stacks on heating, as mentioned above in the case of the film on second heating run. However, in this case the steep increases in the lamellar thickness and the long period should be also attributed to the newly produced lamellar stacks with larger lamellar thicknesses and long periods originated from melting and recrystallization rather than the melting of smaller and/or imperfect crystallites in the lamellar stacks with temperature, because the apparent crystallinity index does not decrease up to the melting point (Fig. 6) and the increase in the lamellar thickness is accompanied with the increase in the linear crystallinity within the lamellar stacks in this temperature domain as shown in Fig. 9. Therefore, above 150 °C the newly lamellar stacks with larger lamellar thicknesses and lateral crystallite sizes must be produced via melting and recrystallization, although a part of thermally stable existing lamellae may be thicken with increasing temperature.

In conclusion, on first heating run the PVA film goes through recrystallization and/or rearrangement of existing crystallites without the increase in the crystallite size below 150 °C, and melting and recrystallization with the crystallite size increase in both directions parallel and perpendicular to the chain axis above 150 °C.

4.3. Role of boric acid on melting of PVA

For the films with boric acid, the same SAXS/WAXD simultaneous scattering experiments were performed on first heating run. Figs. 11 and 12 show the apparent crystallinity indexes and the lateral crystallite sizes in the direction perpendicular to the chain direction with temperature, respectively. Corresponding values of the PVA without boric acid on first heating run are also included in the figures, as the PVA film dried after immersing in the boric acid aqueous solution with 0 wt% boric acid concentration.

The apparent crystallinity index at 50 °C prior to heating decreases with increasing the boric acid concentration in the film, probably due to the effect of boric acid on hindering recrystallization of the PVA films during the dry process after immersing the films in boric acid aqueous solutions. In previous paper [4], we found that an appropriate amount of smaller and/or imperfect crystallites may dissolve in water even at room temperature, although the crystallinity index is recovered to the previous value after drying the film by recrystallization during the dry process. We will discuss again on this matter in Discussion section.

Fig. 13 shows the scattering invariants for the films with boric acid. Figs. 14a, b and 15 show the long period, the lamellar thickness and the consequence linear crystallinity in the lamellar stacks on first heating run, respectively.

As shown in Fig. 11, for the films with boric acid, recrystallization and/or rearrangement of exiting crystallites also occur between 100 °C and 150 °C in the same way as the case of the PVA film without boric acid. In this temperature domain the lateral crystallite size (Fig. 12) and the lamellar thickness (Fig. 14(b)) also remain constant, implying that recrystallization and/or rearrangement of existing crystallites occur without the increase in the crystallite sizes in the lateral and the parallel directions to the chain axis as the same case as the PVA without boric acid. Fig. 11 also indicates that the apparent crystallinity index of the film with boric acid decreases steeply at a lower temperature above 150 °C with

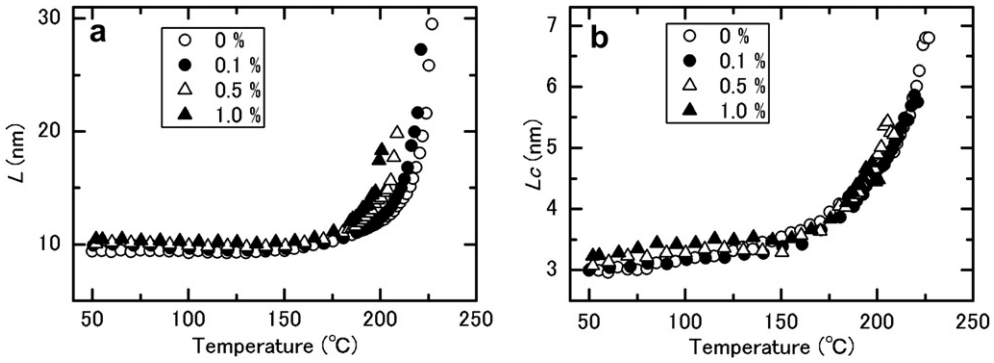

Fig. 14. Long periods (a) and the lamellar thicknesses (b) of the PVA films with various boric acid contents dried after immersing in aqueous solutions with various boric acid concentrations shown in the figure.

increasing the boric acid concentration. That is to say, the melting temperature decreases with increasing the boric acid concentration in the film, as shown in Fig. 5(a). Furthermore, as shown in Figs. 12 and 14b, above 150 °C, the increases in the lateral crystallite size and the lamellar thickness are inhibited for the films with boric acid, especially with the boric acid concentrations in solutions of 0.5 wt% and 1.0 wt%, implying that only melting of existing crystallites takes place, whereas recrystallization does not occur with the growth of the crystallite size in the lateral and the chain directions of the lamellar for the films containing boric acid fully. For the films containing boric acid fully, a moderate increases in the lamellar thickness must be mainly attributed to the melting of smaller crystallites in the lamellar stacks, because above 150 °C it can be observed that the apparent crystallinity index decreases substantially, and the increase in the linear crystallinity within the lamellar stacks levels off, as shown in Figs. 11 and 15. No appearance of recrystallization with the increase in the crystallite size also explains the decrease in the melting point for the PVA film with boric acid, as mentioned above relating to Fig. 5(a), because the crystallite growth induced with melting and recrystallization leads to the delay of the final melting point. It is considered that boric acid hinders recrystallization accompanied with the increase in the crystallite size in both directions parallel and perpendicular to the molecular chain direction by cross-links formed in the amorphous regions nearby crystallites, as a result of reactions of boric acid to the PVA molecular chains.

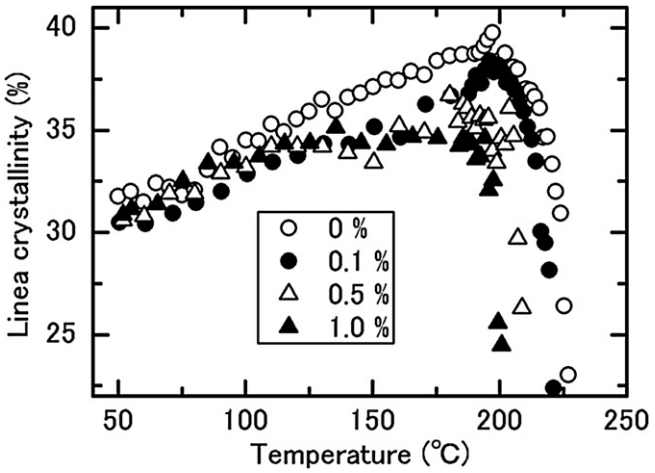

Fig. 15. Linear crystallinity in the lamellar stacks of the PVA films with various boric acid contents dried after immersing in aqueous solutions with various boric acid concentrations shown in the figure.

As shown in Figs. 13 and 15, the unexpected invariant changes below 150 °C and the increase in the linear crystallinity within the lamellar stacks above 80 °C can be also observed for all films irrespective of the boric acid concentration, attributed to water evaporation during heating, as discussed in Discussion section later. The invariant of the film with boric acid at 50 °C decreases with the boric acid concentration in the film, also indicating that recrystallization during the dry process is inhibited with reactions of boric acid to the molecular chains of the PVA resulted in cross-linking points after immersing the film in boric acid aqueous solution, as mentioned in the case of the apparent crystallinity index at 50 °C accessed by WAXD measurements (Fig. 11). The further increases in the invariant and the linear crystallinity within the lamellar stacks cannot been observed for the films with a high boric acid concentration above 150 °C, also indicating that for the films containing boric acid fully, melting occurs only and recrystallization with the growth of crystallites does not take place in the direction parallel to the chain axis.

Both WAXD and SAXS results indicate that for the films with boric acid recrystallization and/or rearrangement of exiting crystallites occur below 150 °C in the same way as the PVA film without boric acid. However, melting and recrystallization with the increase in the crystallite size is inhibited above 150 °C with the cross-linking points via reactions of boric acid to the PVA molecular chains, because the cross-linking points slow down the molecular motion, as described with the DSC results, and must be excluded out of the crystalline alignments of the molecular chains.

5. Discussion

5.1. Water evaporation on first heating run

On first heating run, the scattering invariant does not substantially change with temperature in the temperature range of 80–150 °C irrespective of the boric acid concentration in the film, as shown in Fig. 13. This is schematically shown in Fig. 16, which describes the selected 1-D SAXS profiles on first heating run for the PVA film without boric acid. The constancy in the scattering invariant between 80 °C and 150 °C cannot be interpreted with the possible explanations describing the heating processes of general semi-crystalline polymers [21–26]. We attempt to explain this behavior with water evaporation out of the films on heating.

It is well known that PVA is swollen with water [27–30]. Even under ambient condition, a moderate amount of water may be contained in the film. Fig. 17 shows the DSC endothermic curve of the film used in this study, which was stored under ambient condition for 1 week. The apparent *Tg* lies at about 40 °C, implying

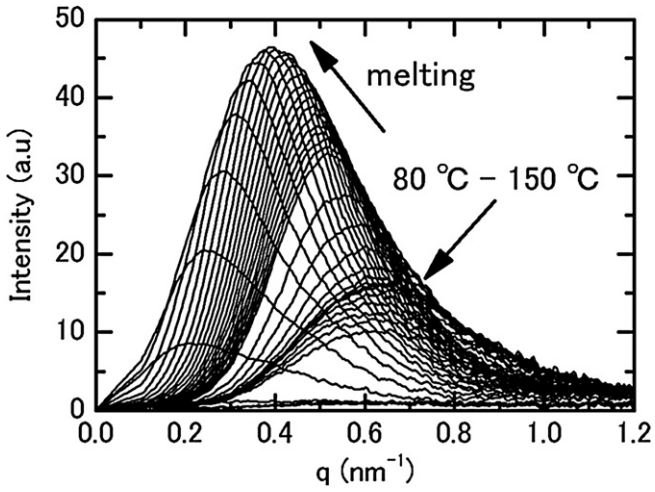

Fig. 16. SAXS one-dimensional scattering profiles of the PVA film without boric acid on first heating run.

that the *Tg* is substantially reduced compared to that of the film after drying in a vacuum oven at 60 °C for 12 h, 67 °C as shown in Fig. 5(a), which was measured immediately after drying. Furthermore, Fig. 17 also indicates the broad endothermic peak lied at about 130 °C, which is starting from about 80 °C. This broad endothermic peak must be attributed to water evaporation, because this endothermic peak disappears for the film measured immediately after drying under vacuum. Furthermore, for the PVA film examined in this study, vapor constituent was also investigated on heating by using gas chromatography/mass spectrometry, indicating that water is evaporated out of the film in the temperature range of 60–140 °C, which is consistent with the endothermic peak area. Therefore, we should conclude that the PVA film is swollen with water even under ambient condition.

Water evaporation starting from 80 °C can be also revealed with the SAXS analysis using the one-dimensional correlation functions. Fig. 18 shows the expanded views of the long periods of the films with various boric acid concentrations on first heating run, as shown in Fig. 14(a). Clearly, the long periods decrease with temperature in the temperature range of 80–150 °C. The inset of this figure shows the thicknesses of amorphous regions in the lamellar stacks on first heating run, describing that in the temperature range of 80–150 °C the long period decrease should be attributed to the thickness decrease in the amorphous regions only, because the lamellar crystallite thicknesses gradually increase in this temperature domain, as shown in Fig. 14(b). In particular, this decrease in the amorphous region thickness starting from about 80 °C can be clearly observed in the case of the PVA without boric acid, as shown in the inset of Fig. 18. These behaviors can be explained by water evaporation out of the amorphous regions.

As indicated in our previous paper, only amorphous regions of the PVA film are swollen with water, whereas water cannot penetrate in crystalline regions [3]. Therefore, ambient water can be absorbed into only the amorphous regions in and among the lamellar stacks under ambient condition, leading to the increase in the amorphous region thickness in the lamellar stacks with swelling, as compared to that in a dried state. On first heating run, water begin to be evaporated out of the amorphous regions above 80 °C, leading to the decrease in the amorphous region thickness accompanied with the increase in density of these regions. This thickness decrease in the amorphous regions also explains the increase in the linear crystallinity within the lamellar stacks above 80 °C without substantial structural changes such as recrystallization, as mentioned above relating to Fig. 9.

These water evaporation behaviors can also explain the unexpected scattering invariant changes in the temperature domain of 80–150 °C on first heating run, as schematically described in Fig. 13. The moderate increase in the scattering invariant up to about 80 °C should be ascribed to the larger difference in the thermal expansion coefficients between the amorphous and the crystalline regions above *Tg* compared to that below *Tg*, because *Tg* dramatically decreases below 80 °C with water as shown in Fig. 17. In the temperature domain of 50–80 °C, the thermal expansion coefficient of the amorphous regions is much larger than that of crystalline ones, leading to the substantial density difference between the amorphous and the crystalline regions and consequently to a large increase in the invariant compared to that below *Tg*, as mentioned above about the linear increase in the invariant with a larger linearity constant above 75 °C for the film on second heating run in Fig. 10.

The constancy of the invariant in the temperature range of 80–150 °C can be explained mainly with the increase in density of the amorphous regions accompanied with the thickness decrease in these regions with water evaporation on heating. The increase in

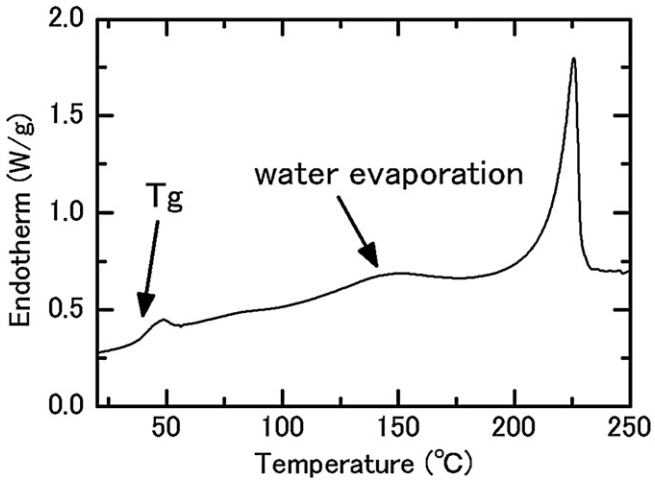

Fig. 17. DSC endothermic curve of a PVA film without boric acid stored under ambient condition for 1 week.

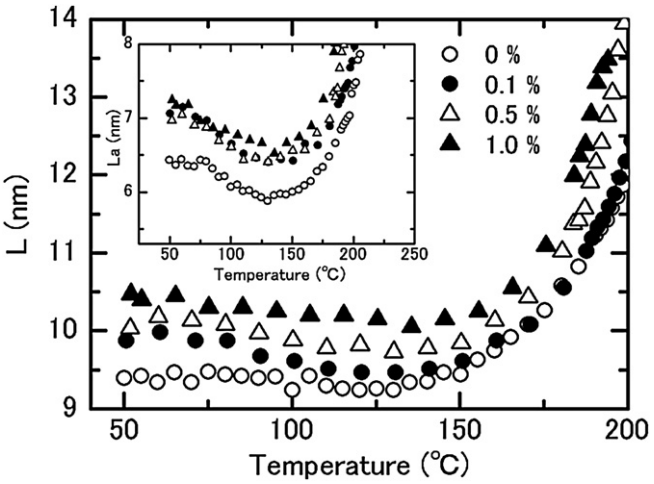

Fig. 18. Long periods of the PVA films with various boric acid contents dried after immersing in aqueous solutions with various boric acid concentrations shown in the figure. Inset; the thicknesses of the amorphous regions in the lamellar stacks for the same specimen.

density of the amorphous regions with water evaporation leads to the decrease in the density difference between the amorphous and the crystalline regions, and consequently to the decrease in the invariant, as expected from Eq. (7). This decrease in the scattering invariant is compensated by the increase in the scattering invariant attributed to recrystallization and/or rearrangement of existing crystallites, which is confirmed by WAXD as shown in Figs. 6 and 11. As a result, it is considered that the scattering invariant remains constant in the temperature domain of 80–150 °C. At about 150 °C, water evaporation is completed as shown in the DSC endothermic curve (Fig. 17), leading to the steep increase in the scattering invariant again, which is due to a larger density difference between the amorphous and the crystalline regions, and melting and recrystallization, for the PVA without boric acid. As mentioned above, for the PVA films with boric acid the further increase in the scattering invariant is not observed, because only melting takes place without recrystallization.

5.2. Effects of boric acid on hindering recrystallization

As shown in our previous paper, for the PVA used in this study, a part of crystallites with smaller sizes and/or imperfect ordering dissolves in water even at room temperature [4], resulted in a lower crystallinity index of the film in water compared to that in a dried state. In previous paper, we found that the film has a crystallinity index of 22–26% in water, retaining the previous value, 30–35% during drying the film [4]. Therefore, it is considered that recrystallization takes place during the dry process. However, the crystallinity indexes in the films with boric acid are lower than that of the PVA without boric acid after drying the films, as shown in Fig. 11. It may be expected that boric acid hinders recrystallization of the PVA chains during a dry process [31].

As described above, the PVA film used in this study goes through the substantial structural changes on first heating run, such as recrystallization and/or rearrangement of existing crystallites above 100 °C, and melting and recrystallization with the crystalline size increase above 150 °C, if the film contains no boric acid. This means that the crystallinity index of the film without boric acid cannot be simply determined with the endothermic peak area accessed by DSC. Fig. 19 shows the crystallinity indexes of the films with various boric acid concentrations which are determined with the endothermic peak areas obtained in Fig. 5(a). The crystallinity index of the PVA without boric acid is about 45%, substantially larger than our previous reported one, 32%, which was determined by the density obtained with the floating method and was consistent with the value of 34% derived from an X-ray method similar to that used in this study [32]. In this study, the crystallinity index of the PVA without boric acid is 33% at 50 °C prior to first heating run as described in Fig. 6, consistent with the previous one very well. These results indicate that the crystallinity index of the PVA without boric acid is 32–34% and that determined by DSC is overestimated mainly for melting and recrystallization on heating.

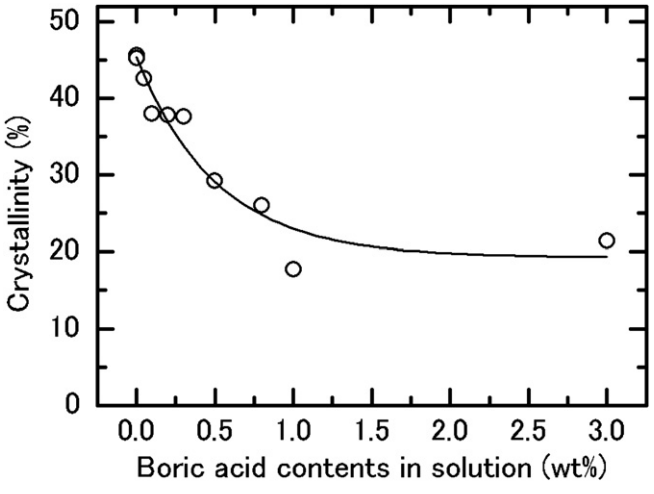

Fig. 19. Crystallinity indexes derived from DSC endothermic peak areas of the PVA films with various boric acid contents dried after immersing in aqueous solutions with various boric acid concentrations shown in the figure. The solid line is drawn to guide the eye.

Boric acid hinders recrystallization with cross-links in the amorphous regions, as described above. Fig. 19 also indicates that the crystallinity index determined with DSC decreases with increasing the boric acid content in the film and remains constant above a boric acid concentration of 1 wt%, implying that a high degree of cross-links hinders completely recrystallization on heating. The crystallinity index of the films containing boric acid fully is about 20%, consistent with the values determined with X-ray method for the film in water obtained in our previous paper (20–26%) and that of the film dried after immersion in the boric acid aqueous solution with the boric acid concentration of 1 wt% (27.5%). These facts may indicate that DSC can determine the crystallinity indexes of the PVA containing boric acid fully without the effects of melting and recrystallization on heating, although recrystallization and/or rearrangement of the crystallites occur above 100 °C as shown in Fig. 11.

As shown in Fig. 5(b), *Tg* increases moderately with boric acid concentration in solution up to 3 wt%, indicating that the cross-linking density in the film also increases with boric acid concentration in solution up to 3 wt%. However, it is suggested that the film should be immersed in a boric acid aqueous solution with a boric acid concentration above 1 wt% for hindering fully recrystallization during dry processes and on heating.

6. Conclusion

We have investigated the role of boric acid as a cross-linking agent for a PVA film when the film is immersed in boric acid aqueous solutions. DSC measurements were performed on the films dried after immersing in boric acid aqueous solutions with various boric acid concentrations, indicating that the PVA films with boric acid exhibit the higher glass transition temperatures than that of the PVA without boric acid. We found that boric acid penetrating into the film slows down the PVA molecular motion.

Furthermore, simultaneous SAXS/WAXD measurements were performed on the melting processes of the PVA films with and without boric acid. First, we investigated the melting process of the PVA film without boric acid. For the PVA film without boric acid we found that the crystallite size is enlarged in both directions parallel and perpendicular to the chain axis via melting and recrystallization above 150 °C. Second, the same simultaneous SAXS/WAXD experiments were applied to the investigation on the melting processes of the PVA films containing various boric acid contents. It was found that recrystallization with the crystallite size increase does not take place for the PVA containing boric acid fully.

These results indicate that boric acid reacts to the PVA chains in the amorphous regions, resulted in cross-linking points for the PVA chains. These cross-linking points inhibit recrystallization during a dry process after immersing the film in boric acid aqueous solutions, and melting processes, because the cross-linking points slow down the molecular motion and must not be included in the crystalline alignments of molecular chains.

Acknowledgement

The authors wish to thank Dr. S. Sasaki, Dr. H. Masunaga and Dr. H. Ogawa of the Japan Synchrotron Radiation Research Institute (JASRI) and Dr. Y. Sugino of Nitto Denko Corporation for their support on our experiments at SPring-8. The synchrotron radiation experiments were performed at the BL40B2 in the SPring-8 with the approval of JASRI (Proposal No. 2009A1280).

References

[1] Sakurada I. Polyvinyl alcohol fibers. New York: Marcel Dekker; 1985.
[2] Finch CA. Polyvinyl alcohol: preparation and application. London: Wiley; 1973.
[3] Miyazaki T, Hoshiko A, Akasaka M, Shintani T, Sakurai S. Macromolecules 2006;39:2921.
[4] Miyazaki T, Hoshiko A, Akasaka M, Sakai M, Takeda Y, Sakurai S. Macromolecules 2007;40:8277.
[5] Miyasaka K. Adv Polym Sci 1993;108:91.
[6] Zwick MM. J Appl Polym Sci 1965;9:2393.
[7] Ochiai H, Shimizu S, Tadokoro Y, Murakami I. Polymer 1981;22:1456.
[8] Shibayama M, Sato M, Kimura Y, Fujiwara H, Nomura S. Polymer 1988;29:336.
[9] Wu J, Schultz JM, Yeh F, Hsiao BS, Chu B. Macromolecules 2000;33:1765.
[10] Wu J, Schultz JM, Samon JM, Pangelinan AB, Chuah HH. Polymer 2001;42:7131.
[11] Nogales A, Sics I, Ezquerra TA, Denchev Z, Balta Calleja FJ, Hsiao BS. Macromolecules 2003;36:4827.
[12] Strobl GR, Schneider MJ. Polym Sci Part B Polym Phys 1980;18:1343.
[13] Hsiao BS, Sauer BB, Verma RK, Zachmann HG, Seifert S, Chu B, et al. Macromolecules 1995;28:6931.
[14] Hsiao BS, Gardner KH, Wu DQ, Chu B. Polymer 1993;34:3986.
[15] Hsiao BS, Gardner KH, Wu DQ, Chu B. Polymer 1993;34:3996.
[16] Verma RK, Velikov V, Kander RG, Marand H, Chu B, Hsiao B. Polymer 1996;37:5357.
[17] Verma R, Marand H, Hsiao B. Macromolecules 1996;29:7767.
[18] Santa Cruz C, Stribeck N, Zachmann HG, Balta Calleja FJ. Macromolecules 1991;24:5980.
[19] Endo R, Amiya S, Hikosaka MJ. Macromol Sci Part B Phys 2003;42:793.
[20] Holland BJ, Hay JH. Polymer 2001;42:6775.
[21] Jonas AM, Russell TP, Yoon DY. Macromolecules 1995;28:8491.
[22] Jonas AM, Russell TP, Yoon DY. Colloid Polym Sci 1994;272:1344.
[23] Fougnies C, Damman P, Villers D, Dosiere M, Koch MHJ. Macromolecules 1997;30:1385.
[24] Fougnies C, Damman P, Dosiere M, Koch MHJ. Macromolecules 1997;30:1392.
[25] Flores A, Pieruccini M, Nochel U, Stribeck N, Balta Calleja FJ. Polymer 2008;49:965.
[26] Gehrke R, Riekel C, Zachmann HG. Polymer 1989;30:1582.
[27] Higuchi A, Iijima T. Polymer 1985;26:1207.
[28] Ruiz J, Mantecon A, Cadiz VJ. Polym Sci Part B Polym Phys 2003;41:1462.
[29] Hodge RM, Edward GH, Simon GP. Polymer 1996;37:1371.
[30] Hodge RM, Edward GH, Simon GP, Hill AJ. Macromolecules 1996;29:8137.
[31] Ohishi K, Itadani T, Hayashi T, Nakai T, Horii F. Polymer 2009;51:687.
[32] Miyazaki T, Katayama S, Funai E, Tsuji Y, Sakurai S. Polymer 2005;46:7436.